RSC Advances




ROYAL SOCIETY OF CHEMISTRY

www.rsc.org/advances

Journal Name

RSCPublishing

ARTICLE

# Poly (4-methyl-1-pentene-1) / Alkylated Graphene Oxide Nanocomposites：The Emergence of a New Crystal Structure

Cite this: DOI: 10.1039/x0xx00000x

Received 00th January 2012,
Accepted 00th January 2012

DOI: 10.1039/x0xx00000x

www.rsc.org/

Li-yang Xu[a], Huai-wen Yan[a], Lei Gong[b], Bo Yin[a]*, Ming-bo Yang[a]

The modified graphene oxide (GO) not only offers wrinkled structure but also has a possibility to transform the crystal structure, which makes a potential application of high performance polymer/filler composites. In this work, alkylated graphene oxide (GO-ODA) is obtained via mutual electrostatic interaction between the epoxide group of GO and the amine group of octadecylamine (ODA). Then nanocomposites are obtained via introducing different content of GO-ODA to poly (4-methy-l-pentene-1) (PMP or TPX) with solution approach. It is found that the obtained GO-ODA has no effect on crystallinity of TPX. It is worth noting that GO-ODA makes the crystal structure changed. GO, as a kind of nanofiller, is used to change crystal structure of polymer/filler composites for the first time, which is an important finding and obviously provides a good example to widen the application of GO.

## Introduction

Poly (4-methy-l-pentene-1) (PMP), also called TPX, is a semicrystalline polyolefin that is an important industrial material with many different properties, such as heat resistance (high melting point), light weight (low density), release properties (low surface tension) and excellent clarity. PMP presents a complex polymorphic behavior, thus five different crystalline forms have been reported. They can be obtained from crystallization in semidilute solutions depending on the solvent and the thermal history of the solutions.[1, 2] Form I is the most stable crystalline form, and can be obtained from the melt or from crystallization in high boiling solvents.[2-4] Form I is characterized by chains in 7/2 helical conformation, packed in a tetragonal unit cell with axes a = 18.66 Å and c = 13.80 Å according to the space group $P\bar{4}$. Slight deviations from the uniform 7/2 helical conformation has been suggested for Form I, and the chains, in the Form I, distort in the space group $P4\bar{b}2$ in a successive refinement of the structure.[4] For the Form II, Takayanagi et al.[5] reported, a tetragonal unit cell with axes a = 19.16 Å and c = 7.12 Å with chains in 4/1 helical conformation, according to X-ray diffraction spectra on single crystal mats. Afterwards Charlet, G et al. found that a chain packing in a monoclinic unit cell with a = 10.49 Å, b = 18.89 Å and c = 7.13 Å and γ = 113.7° in the same 4/1 helical conformation.[6, 7] Herein, the Form II has two kinds of unit cell structure. According to the unit cell previously proposed by Takayanagi et al,[5] Charlet et al.[2] have reported that the Form III is tetragonal unit cell with chains in 4/1 helical conformation, and its lattice parameters are axes a = 19.38 Å and c = 6.98 Å. De Rosa et al. proposed that the Form III was characterized by a tetragonal unit cell (a = 19.46 Å, c = 7.02 Å), with 4/1 helical conformation according to the space group $I4_1$, which can be obtained from xylene cyclohexane solutions.[8, 9] Charlet and Delmas[10] have proposed that the unit cell parameters of the Form IV, which is characterized by chains in 3/1 helical conformation[11] with axes a = 22.17 Å and c = 6.69 Å in a hexagonal unit cell. The Form IV can be prepared by annealing Form I above 200 °C under pressure (4500 atmospheres)[12] or from cyclopentane solutions.[10] The Form V has been obtained in cyclohexane gels[13] and by crystallization in cyclohexane and carbon tetrachloride solutions,[1] but there has been no report about the detailed structural analysis up to now.

Graphene oxide (GO), as an excellent material, has attracted tremendous attention in recent years.[14, 15] It is a compound of carbon, oxygen, and hydrogen in variable ratios, formerly called graphitic oxide or graphitic acid. The structure and properties of graphene oxide depend on the particular synthesis method, degree of oxidation[16-19] and how it typically preserves the layer structure of the parent graphite, although the layers are buckled and the interlayer spacing is much larger than that of graphite.[16] The as obtained GO sheet has a lot of epoxy, hydroxyl and carboxyl functional groups on its basal plane. So graphene oxide can disperse readily in most polar solvents such as water, breaking up into macroscopic flakes, which are mostly one layer thick. However, the graphene oxide is polar, therefore, it doesn't get a good dispersion in the non-polar polymer. Despite this, GO has been developed over the course of small molecule organic chemistry due to the ionization of carboxyl groups, therefore we can change the polarity of GO. Herein researchers have introduced graphene oxide to the surface of amorphous glass fiber (GF) to induce the interfacial crystallization between semi-crystalline polymer and GF.[20] This motivated us to ask if GO could be dispersed in TPX via the electrostatic assembling method, such as alkylated graphene oxide, which may enhance the nucleation ability on semicrystalline polymers. And the wrinkled structure of

modified GO may change the crystalline structure on semi-crystalline polymers.

Many researchers have studied the crystal structure, morphology and crystallization dynamics of TPX as a test material in many investigations. And some have investigated the properties of the blends that consisted of the TPX and some organic[21, 22] or inorganic nano-fillers.[23, 24] To date, almost no people have studied the effect of graphene on TPX. Therefore, in this work, we first carry out the modification of GO with octadecylamine (ODA) via electrostatic self-assembly. After the GO-ODA has been dispersed in TPX by solution blends, the crystallization behavior of TPX/GO-ODA nanocomposites is investigated. Our goal is two-folds. One is to find out if the GO could change crystal structure of TPX, and the other is to explore some new application of GO.

## Experimental

### Materials and preparation of the samples

In this paper, the PMP or TPX, was purchased from Mitsui Chemicals Americal, Inc. with Physical and mechanical properties in the table 1. The solvent cyclohexane was chemically pure (99.5%) and was used without further purification. The graphite flake was obtained from Research Institute of Shenghua, Changsha, Hunan, China.

Table 1. Physical and mechanical properties of PMP.

| Melting Temperature($T_m$) | Melt flow rate (260 $^oC$ /5 kg) | Dielectric constant | Transparency | Density |
|---|---|---|---|---|
| 232 $^oC$ | 26 g/10 min | 2.12 | 94% | 0.833 g/cm$^3$ |

The graphene oxide (GO) was obtained via the "Improved Hummers′ method",[25] of which oxidation procedure ($KMnO_4$ and a 9:1 mixture of concentrated $H_2SO_4$/$H_3PO_4$) could be used to prepare improved GO with fewer defects in the basal plane as compared to the GO prepared by the Hummers′ method.[26] For surface modification, graphene oxide was dispersed in 100 mL distilled water (2 mg/mL) via ultrasonication with a KQ-400KDB ultrasonicator. Then, the graphene oxide solution was centrifuged for 30 min at 4000 rpm to remove the unexfoliated graphene oxide. Octadecylamine (ODA 900 mg) was dissolved in ethanol and the solution was added into the graphene oxide solution followed by stirring at 90 °C for 20 h. The nucleophilic substitution occurred through the amine functionality of ODA to the epoxy functionality of GO. The final product was washed with water-ethanol mixture to remove the excess ODA adsorbed on the surface of the modified graphene (GO-ODA). The black powders were dried under vacuum at 50 °C for 24 h.[27, 28]

The present results show that TPX can be dissolved in cyclohexane.[1] So the poly(4-methylpentene-1) was dissolved in the three-necked flask with cyclohexane, which was maintained constant temperature of about 50 $^oC$. At the same time, the modified graphene solution, after ultrasonication for 30 min, was added to the above three-necked flask. When the TPX dissolved perfectly, after ultrasonicating for 60 min, the solution was poured into a glass template, evaporating solvent. Finally, we can get the product. In this research, the proportions of GO-ODA in the nanocomposites are: 0.1 wt%, 0.2 wt%, 0.5 wt%, 1.0 wt%.

### Characterization

The exfoliation quality of GO–ODA nanosheets in the TPX matrix was observed with a Tecnai G2 F20 S-TWIN transmission electron microscope (TEM). The GO-ODA was dispersed in cyclohexane solution of TPX, and collected on 200-mesh copper grids. GO and GO–ODA were analyzed with a NICOLET 6700 Fourier-transform infrared spectroscopy (FT-IR). Thermo-gravimetric analysis (TGA) of GO-ODA was carried out on a TGA/DSC with a heating rate of 10 °C /min over the temperature range of 30-700 °C in a nitrogen atmosphere. The chemical character of the GO-ODA was analyzed by a XSAM800 X-ray photoelectron spectroscopy (XPS).

The calorimetric properties of the samples were studied by a differential scanning calorimeter (DSC TA Q20). The apparatus was calibrated with pure indium at various scanning rates. After eliminating any thermal history, each sample was heated-cooled from 40 °C to 250 °C at the rate of 10 °C /min with dry nitrogen gas during the measurements. The heat flow evolved during the scanning process was recorded as a function of temperature.

X-ray diffraction patterns were obtained on a DX-1000 automatic diffractometer operating at a step size of 0.02° with a nickel-filtered Cu Kα radiation.

The $^{13}C$ solid-state cross-polarization magic angle spinning (CP-MAS) NMR studies were conducted using a Bruker AVANCE III spectrometer on the polymer samples recovered after crystallization. In this paper, these NMR CP-MAS data were compared with the characteristic NMR patterns reported in the literature[29, 30] for the different crystalline forms of this polymer for assignments of the different crystalline forms that were generated in a given experiment.

## Results and discussion

In this paper we get the GO-ODA without the use of any catalyst/reducing agent. The grafting of ODA on GO is realized via electrostatic self-assembly, as illustrated in Figure 1. Firstly graphite flake is oxidized using a mixed $KMnO_4$, $H_2SO_4$ and $H_3PO_4$ solution, as described in the experiment part. GO sheet is negatively charged due to the presence of oxygen functional groups such as phenolic hydroxyls and carboxylic acids. By simply mixing the aqueous suspension of ODA and GO colloid solution, the positive charged ODA can be successfully graft to the negatively charged GO via electrostatic self-assembly strategy, which could be demonstrated by FTIR spectra, TEM observation and XPS spectra as follows.



 

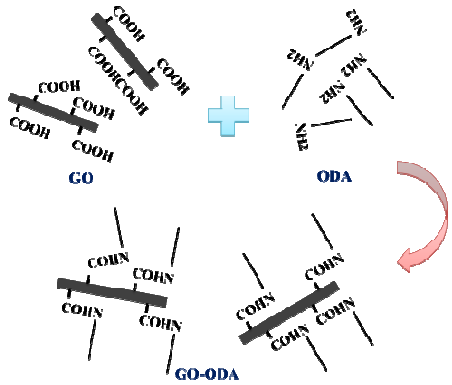


Figure 1. Schematic representation of the grafting of ODA to GO via electrostatic self-assembly.

The TEM images of GO-ODA sheets from the solution consisted of cyclohexane and TPX was shown in Figure 2. Everyone can clearly see that GO-ODA has lamellar structure and wrinkled structure with microcosmic distortions as the research mentioned.[26]

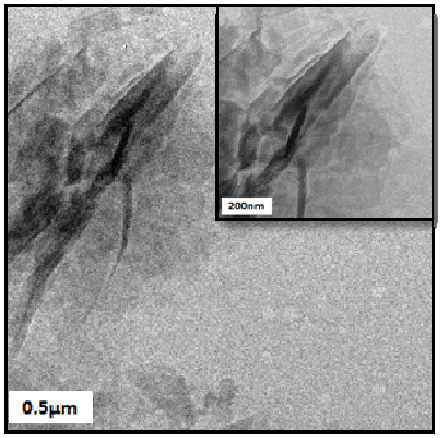


Figure 2. The TEM image of GO-ODA.

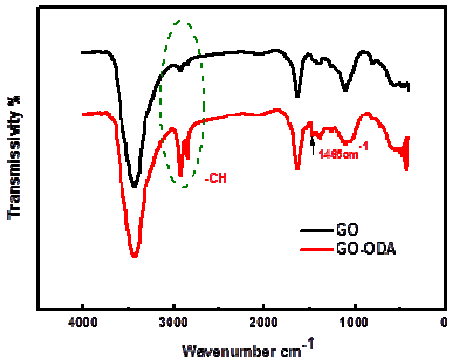


Figure 3. FTIR spectra of GO and GO-ODA.

In addition, FTIR spectra, as a powerful tool for the characterization of graphene and its derivatives, is also employed to demonstrate the successful grafting of ODA on GO. Figure 3 shows the FTIR spectra of pure graphene oxide and GO-ODA. The typical peaks of GO appear at 1710 $cm^{-1}$ (C=O carboxyl stretching vibration), 1685 $cm^{-1}$ (C=C in aromatic ring) and 1385 $cm^{-1}$ (C–OH stretching). Moreover, the wide peak appearing at 3000–3700 $cm^{-1}$ could be assigned to the hydroxyl groups. The emergence of peaks at ~2900 $cm^{-1}$, corresponding to C-H stretching vibrations of CH3, CH2 and CH groups in GO-ODA indicates the successful modification of the graphene oxide, which obviously changes the polarity of GO.

XPS is employed to evaluate the chemical bonds formed on the surface of GO after its functionalization with ODA. Typically, the C 1s peak region of GO-ODA can be fitted into four curves as shown in Figure 4. The binding energies at 284.5 eV, 286.6 eV and 287.8 eV are assigned to unoxidized graphite carbon skeleton (C–C), hydroxyl group (C–OH) and epoxide group (–C–O–C–), respectively, which indicates a considerable degree of oxidation with four components. However, in the XPS spectrum a new peak at 285.2 eV corresponding to C–N appears, demonstrating the reaction of GO with ODA.

As shown in Figure 5, there is no mass loss below 100 °C, which indicates enhanced hydrophobicity that minimizes the amount of absorbed water. From 160 °C to 180 °C, there is a gradual mass loss of ~10%, which is ascribed to the decomposition of physically bonded ODA.[31] These ODA molecules may be positively charged and electrostatically bonded with negatively charged carboxylic groups, which prevents them from being washed away by ethanol. Previous studies showed that the decomposition of chemically bonded amine occurs at the temperature range of 200-500 °C.[32-34] Therefore, the high weight loss rate of GO-ODA at 365 °C is due to the decomposition of covalently bonded ODA, together with the decomposition of GO.

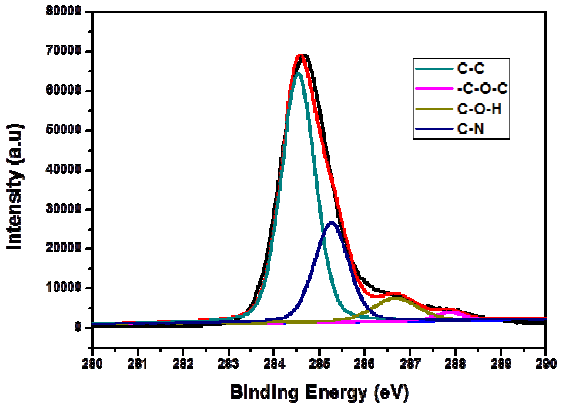


Figure 4. Carbon 1s XPS spectra of GO–ODA.

Differential scanning calorimetry (DSC) was used to study the melting and crystallization behavior of the samples with different loadings of the fillers. And some parameters are presented in Table 2. It is worth noting that twin peaks of melting curve transform to single peak with the increasing content of GO-ODA in the Figure 6 (a). As can be seen from Figure 6 (b), the crystallization peaks of samples have not shifted and are centred at about T=211.6 ± 0.6 °C. Furthermore these parameters (melting point, fusion enthalpy) of five samples have a minor difference. These results indicate that GO-ODA has no effect on fusion enthalpy. In other words, GO-ODA makes no contribution to crystallinity of samples.

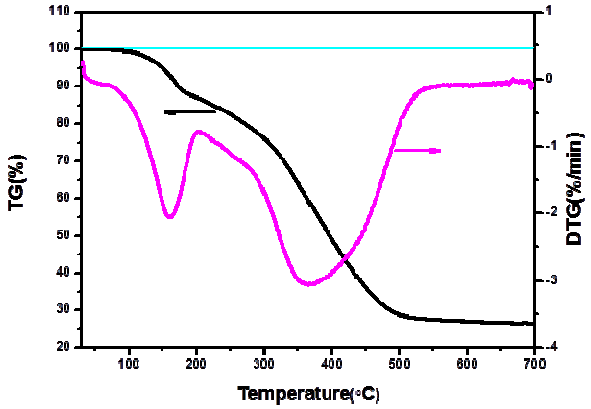


Figure 5. The TGA plots of GO –ODA.

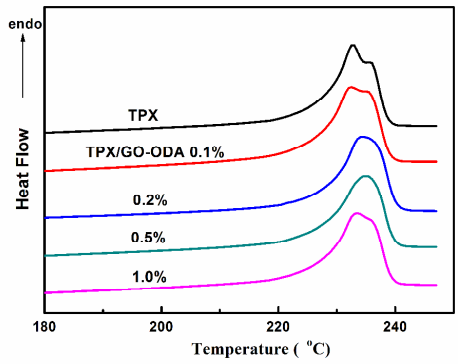


(a)

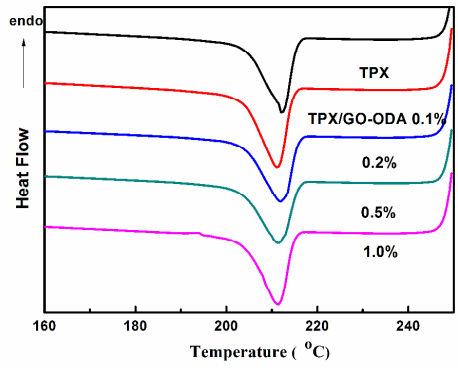


(b)

Figure 6. The DSC curve of TPX/GO-ODA nanocomposites: (a) melting traces; (b) cooling traces.

Table 2. The detailed DSC results of the nanocomposites samples with different nanofillers content.

| | $T_m$ (°C) | $T_c$ (°C) | ΔH (J/g) |
|---|---|---|---|
| TPX | 232.7 | 212.2 | 37.83 |
| TPX/GO-ODA0.1% | 232.5 | 211.2 | 40.88 |
| TPX/GO-ODA0.2% | 234.5 | 211.9 | 36.32 |
| TPX/GO-ODA0.5% | 234.9 | 211.5 | 36.75 |
| TPX/GO-ODA1.0% | 233.4 | 211.4 | 37.92 |

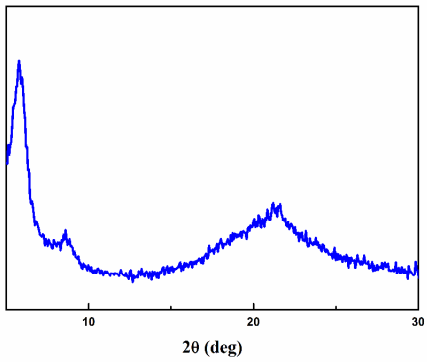


(a)

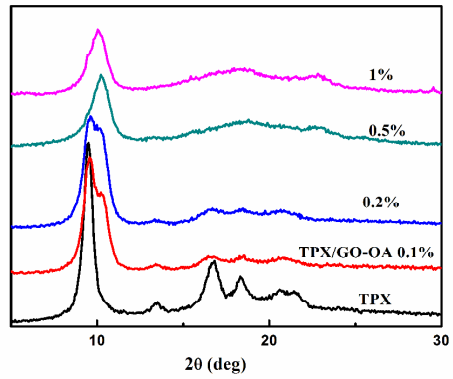


(b)

Figure 7. The X-ray diffraction pattern of samples: (a) GO-ODA; (b) nanocomposites with different nanofiller content.

Table 3. Diffraction angles (2θ Cu Kalpha) and hkl miller indexes of the reflections observed in the X-ray diffraction profiles of TPX of Figure 7 (b).

| 2-Theta (°) | d (Å) | hkl | a-Axis (Å) | c-Axis (Å) |
|---|---|---|---|---|
| 9.524 | 9.279 | 200 | 18.5577 | |
| 13.428 | 6.589 | 220 | 18.6355 | |
| 16.725 | 5.296 | 212 | 18.5577 | 13.7587 |
| 18.328 | 4.837 | 321 | 18.5577 | 14.1445 |
| 20.567 | 4.315 | 113 | 18.5577 | 13.7067 |
| 21.478 | 4.134 | 322 | 18.5577 | 13.8776 |

Table 4. Diffraction angles (2θ Cu Kalpha) and hkl miller indexes of the reflections observed in the X-ray diffraction profiles of TPX/GO-ODA(0.5%&1.0%) of Figure 7 (b).

| TPX/GO-ODA (0.5%) | | | TPX/GO-ODA (1.0%) | | |
|---|---|---|---|---|---|
| 2-Theta (°) | d (Å) | hkl | 2-Theta (°) | d (Å) | hkl |
| 9.930 | 8.900 | 001 | 9.930 | 8.900 | 001 |
| 18.825 | 4.710 | 200 | 18.825 | 4.710 | 200 |
| 22.902 | 3.880 | 210 | 22.902 | 3.880 | 210 |

To further demonstrate the crystal structure of TPX, we investigated the XRD spectra of samples. The intra-gallery space of GO-ODA is enlarged at 2θ = 5.63° in the Figure 7 (a),

which confirms the intercalation of ODA.[27] Figure 7 (b) shows the XRD patterns of the nanocomposites with the different GO-ODA content. We can observe that the GO-ODA has no diffraction peaks on the XRD patterns of nanocomposites. In the present reports, the TPX has five crystalline modification with X-ray diffraction profiles. We can determine that our pure sample is Form I. And the typical diffraction peaks of TPX appear at 2θ=9.524º, 13.428º, 16.725º, 18.328º, and the miller indexes are listed in Table 3. Compare to the diffraction peak of TPX at 2θ = 9.524°, corresponding to crystal plane (200), the peak for TPX/GO-ODA (0.5 wt% & 1.0 wt%) is shifted to 9.930°. And the TPX/GO-ODA (0.1 wt% & 0.2 wt%) nanocomposites remain the crystal face (200). However, intensity of diffraction peaks located at 2θ = 13~25º become weak. In general, with increasing of the GO-ODA content, the diffraction peaks at 2θ = 9.524° offset, and the medium content nanocomposites appear twin diffraction peaks because of the nanofiller. Finally, the results of DSC and XRD demonstrate that the crystal structure transformed.

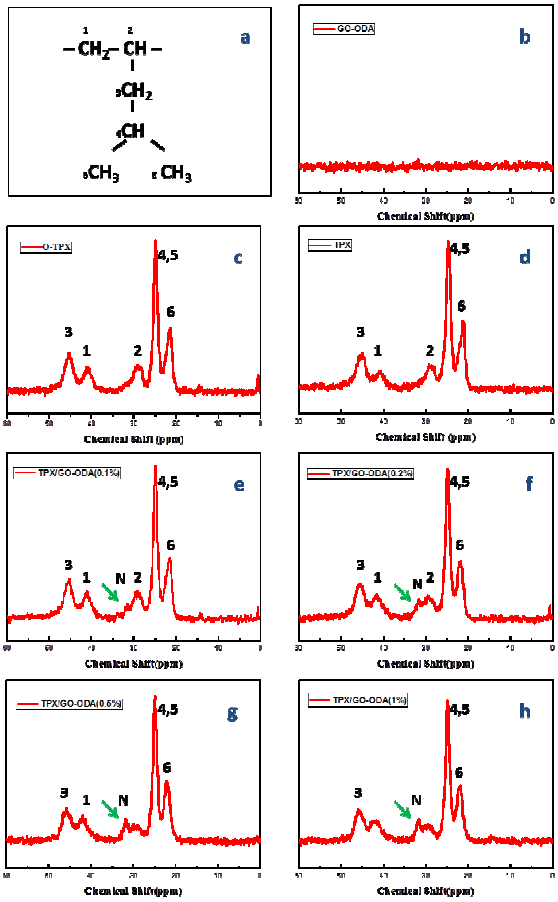


Figure 8. Solid-state $^{13}C$ NMR CP-MAS spectra of TPX/GO-ODA nanocomposites.

In addition, solid-state $^{13}C$ NMR CP-MAS is also employed to further demonstrate the crystal modifications of TPX. Figure 8 shows the solid-state $^{13}C$ NMR CP-MAS spectra of the samples. We can observe that there is no "C" signal of GO-ODA in Figure 8 (b). Based on comparisons with literature,[30] the original polymer and recrystallized polymer from cyclohexane without GO-ODA were crystal modification Form I as shown in Figure 8 (c) and (d). However, the spectra of TPX/GO-ODA nanocomposites in Figure 8 (e~h) appeared a new peak obviously, the CS (or chemical shift) at about 31.0 ppm (the "N" peak). We propose that the GO-ODA is arranged at a specific location in the crystal lattice of TPX, distorts the backbone or side groups of TPX, leading to the crystal structure change. Herein, this result is consistent with the XRD data.

**Mechanism analysis for the emergence of new crystal structure**

In the polymer physics, a conformation is the spatial structure of a polymer determined by the relative locations of its monomers. Thus, a conformation can be specified by a set of n bond vectors between neighbouring backbone atoms. The conformation that a polymer adopts depends on three characteristics: flexibility of the chain, interactions between monomers on the chain, and interactions with surroundings. There are two determinants on conformation of crystalline polymers. One is the interaction between microcrystalline; the other is the repulsive force, Van der Waals forces, electrostatic interaction and hydrogen bonds of non-bonded atoms or groups. Molecular chain of crystal polymer has the most stable conformation, which has different stacking with different crystallization conditions.[35] XRD and $^{13}C$ NMR CP-MAS are effective method for the determination of polymer conformation. In our work, the added GO-ODA changes the interaction between microcrystalline molecules and groups, which makes the conformation of TPX and the molecular chain stacking transformed. This result is showed a new peak at about 31.0 ppm in NMR spectra and a re-formed peak at 2θ = 9.930° in XRD pattern.

The above results demonstrate that the modified GO has no effect on crystallinity of samples. This could be due to the reason that the alkanes group of GO-ODA and the side groups of TPX have entangled. Further, the wrinkled and rough texture of GO-ODA may have an effect on the arrangement of the molecular chain. Obviously, GO-ODA could lead to crystal transition of samples. Therefore, a new crystal structure could be successfully obtained.

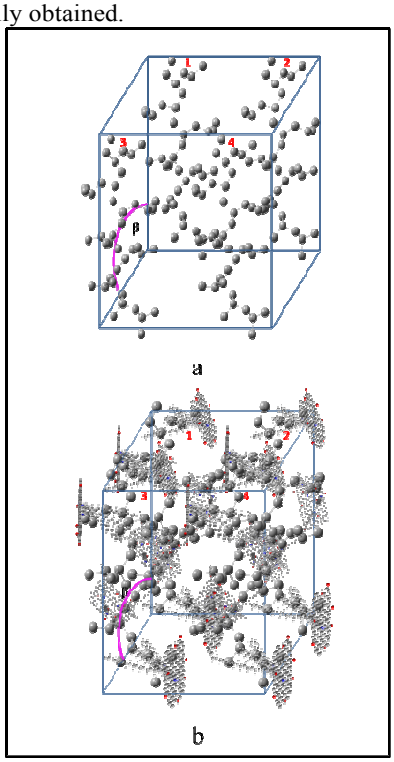


Figure 9. Projections of unit cell: (a) TPX ; (b) TPX/GO-ODA(0.5%, 1%).

For further analysis, we can obtain the simulation unit cell parameters according to the above XRD data and the solid-state $^{13}C$ NMR CP-MAS analysis. The unit cell projections of TPX and TPX/GO-ODA are shown in Figure 9. And the unit cell parameter of TPX is consistent with literatures. We found that TPX/GO-ODA（0.5%，1%） chain packing in a monoclinic unit cell with a = 9.66 Å, b = 6.98 Å and c = 9.1 Å.

## Conclusions

GO-ODA has been successfully obtained via electrostatic self-assembly of the oppositely charged GO and ODA. The as obtained GO-ODA have no effect on crystallinity of TPX. It is worth noting that GO-ODA makes the crystal structure changed. Now we just report preliminary findings, and a great deal of work has to be done to investigate other properties of GO-ODA/TPX nanocomposites based on the different crystal structure. Furthermore, GO has been intensively investigated to improve various properties of polymer composites, and also has been used as the coupling agent of polymer and inorganic fillers. In this work, GO, as a kind of nanofillers, is used to change crystal structure of polymer/filler composites for the first time, which obviously provides a good example to widen the application of GO.

## Acknowledgements

The authors gratefully acknowledge the financial support from the National Natural Science Foundation of China (Contract No. 51273219), State Key Laboratory of Polymer Materials Engineering (Grant No. sklpme2014-3-12) and the Fundamental Research Funds for the Central Universities (No. 2013SCU04A03).

## Notes and references

[a] College of Polymer Science and Engineering, State Key Laboratory of Polymer Materials Engineering, Sichuan University, Chengdu, 610065 Sichuan, China. E-mail: yinbo@scu.edu.cn; Tel: +86-28-85405324

[b] Department of Environment and Chemical Engineering, Dalian University, Dalian, 116622 Liaoning, China.

1. Charlet, G.; Delmas, G. *Polymer* **1984,** 25, (11), 1619-1625.
2. Charlet, G.; Delmas, G.; Revol, J.; Manley, R. S. J. *Polymer* **1984,** 25, (11), 1613-1618.
3. Bassi, I.; Bonsignori, O.; Lorenzi, G.; Pino, P.; Corradini, P.; Temussi, P. *Journal of Polymer Science Part A‐2: Polymer Physics* **1971,** 9, (2), 193-208.
4. Kusanagi, H.; Takase, M.; Chatani, Y.; Tadokoro, H. *Journal of Polymer Science: Polymer Physics Edition* **1978,** 16, (1), 131-142.
5. Takayanagi, M.; Kawasaki, N. *Journal of Macromolecular Science, Part B: Physics* **1967,** 1, (4), 741-758.
6. De Rosa, C. *Macromolecules* **2003,** 36, (16), 6087-6094.
7. Ruan, J.; Thierry, A.; Lotz, B. *Polymer* **2006,** 47, (15), 5478-5493.
8. De Rosa, C.; Borriello, A.; Venditto, V.; Corradini, P. *Macromolecules* **1994,** 27, (14), 3864-3868.
9. Derosa, C.; Auriemma, F.; Borriello, A.; Corradini, P. *Polymer* **1995,** 36, (25), 4723-4727.
10. Charlet, G.; Delmas, G. *Polymer Bulletin* **1982,** 6, (7), 367-373.
11. De Rosa, C. *Macromolecules* **1999,** 32, (3), 935-938.
12. Hasegawa, R.; Tanabe, Y.; Kobayashi, M.; Tadokoro, H.; Sawaoka, A.; Kawai, N. *Journal of Polymer Science Part A‐2: Polymer Physics* **1970,** 8, (7), 1073-1087.
13. Aharoni, S. M.; Charlet, G.; Delmas, G. *Macromolecules* **1981,** 14, (5), 1390-1394.
14. Zhu, Y.; Murali, S.; Cai, W.; Li, X.; Suk, J. W.; Potts, J. R.; Ruoff, R. S. *Advanced materials* **2010,** 22, (35), 3906-3924.
15. Kim, S.; Zhou, S.; Hu, Y.; Acik, M.; Chabal, Y. J.; Berger, C.; de Heer, W.; Bongiorno, A.; Riedo, E. *Nature Materials* **2012,** 11, (6), 544-549.
16. Park, S.; Ruoff, R. S. *Nature nanotechnology* **2009,** 4, (4), 217-224.
17. Han, T. H.; Lee, W. J.; Lee, D. H.; Kim, J. E.; Choi, E. Y.; Kim, S. O. *Advanced Materials* **2010,** 22, (18), 2060-2064.
18. Kim, J.; Cote, L. J.; Kim, F.; Yuan, W.; Shull, K. R.; Huang, J. *Journal of the American Chemical Society* **2010,** 132, (23), 8180-8186.
19. Wang, Z.; Tang, X.-z.; Guo, P.; Duc, X.-s. *Chinese Journal of Polymer Science* **2011,** 29, (3), 368-376.
20. Ning, N.; Zhang, W.; Yan, J.; Xu, F.; Wang, T.; Su, H.; Tang, C.; Fu, Q. *Polymer* **2013,** 54, (1), 303-309.
21. Tao, H. J.; Zhang, J.; Wang, X. L.; Gao, J. L. *J. Polym. Sci. Pt. B-Polym. Phys.* **2007,** 45, (2), 153-161.
22. Tao, H.; Xia, Q.; Jun, S.; Zhang, J.; Wang, X. *Desalination and Water Treatment* **2010,** 17, (1-3), 294-303.
23. Clayton, L. M.; Gerasimov, T. G.; Cinke, M.; Meyyappan, M.; Harmon, J. P. *Journal of nanoscience and nanotechnology* **2006,** 6, (8), 2520-2524.
24. Patil, P. A.; Wanjale, S. D.; Jog, J. P. *E-POLYMERS* **2008**.
25. Marcano, D. C.; Kosynkin, D. V.; Berlin, J. M.; Sinitskii, A.; Sun, Z.; Slesarev, A.; Alemany, L. B.; Lu, W.; Tour, J. M. *ACS nano* **2010,** 4, (8), 4806-4814.
26. Hummers Jr, W. S.; Offeman, R. E. *Journal of the American Chemical Society* **1958,** 80, (6), 1339-1339.
27. Li, W.; Tang, X.-Z.; Zhang, H.-B.; Jiang, Z.-G.; Yu, Z.-Z.; Du, X.-S.; Mai, Y.-W. *Carbon* **2011,** 49, (14), 4724-4730.
28. Kuila, T.; Bose, S.; Mishra, A. K.; Khanra, P.; Kim, N. H.; Lee, J. H. *Polymer Testing* **2012,** 31, (1), 31-38.
29. Fang, J.; Kiran, E. *The Journal of Supercritical Fluids* **2006,** 38, (2), 132-145.
30. De Rosa, C.; Capitani, D.; Cosco, S. *Macromolecules* **1997,** 30, (26), 8322-8331.
31. Lin, Z.; Liu, Y.; Wong, C.-p. *Langmuir* **2010,** 26, (20), 16110-16114.
32. Basiuk, E. V.; Monroy-Peláez, M.; Puente-Lee, I.; Basiuk, V. A. *Nano letters* **2004,** 4, (5), 863-866.
33. Ham, H. T.; Koo, C. M.; Kim, S. O.; Choi, Y. S.; Chung, I. J. *Macromolecular Research* **2004,** 12, (4), 384-390.
34. Compton, O. C.; Kim, S.; Pierre, C.; Torkelson, J. M.; Nguyen, S. T. *Advanced Materials* **2010,** 22, (42), 4759-4763.
35. Sperling, L. H., *Introduction to physical polymer science*. John Wiley & Sons: 2005.



 